Bragg Scattering of Cooper Pairs in an Ultracold Fermi Gas

K. J. Challis, R. J. Ballagh, and C. W. Gardiner

Jack Dodd Centre for Photonics and Ultra-Cold Atoms, Department of Physics, University of Otago, P.O. Box 56, Dunedin, New Zealand

(Received 12 April 2006; published 28 February 2007)

We present a theoretical treatment of Bragg scattering of a degenerate Fermi gas in the weakly interacting BCS regime. Our numerical calculations predict correlated scattering of Cooper pairs into a spherical shell in momentum space. The scattered shell of correlated atoms is centered at half the usual Bragg momentum transfer, and can be clearly distinguished from atoms scattered by the usual single-particle Bragg mechanism. We develop an analytic model that explains key features of the correlated-pair Bragg scattering, and determine the dependence of that scattering on the initial pair correlations in the gas.

DOI: 10.1103/PhysRevLett.98.093002 PACS numbers: 32.80.Cy, 03.75.Ss

Bragg scattering provides a high precision spectroscopic technique that has been adapted from materials science to probe Bose-Einstein condensates [1,2]. In condensate systems, signatures of soliton evolution [3], phase fluctuations [4], center-of-mass motion [5], and vortex structure [6], are accessible due to the velocity selectivity of Bragg spectroscopy. It has been proposed (e.g., [7–12]) that Bragg spectroscopy of an ultracold Fermi gas can provide insight into the Cooper paired regime, and the transition through a Feshbach resonance to molecule formation.

In this Letter we develop Bragg spectroscopy as a probe of ultracold atoms by investigating Bragg scattering of a weakly attractive Cooper paired Fermi gas. Our calculations differ from existing theoretical treatments by: (i) providing explicit solutions for the time evolution of the matter field subjected to a moving optical grating, allowing direct observation of the dynamic response of the gas in momentum space, (ii) investigating in detail the large momentum transfer regime, where the atoms scatter well outside the Fermi sea, and (iii) determining the Bragg spectrum of the Fermi gas in an analogous way to the case for a Bose-Einstein condensate [2,13], by calculating the momentum transfer per atom over a range of Bragg frequencies. The key result we report is Bragg scattering of correlated atom pairs via generation of a Bragg grating in the pair potential.

Our theoretical treatment is based on a mean-field description of a degenerate weakly attractive homogeneous Fermi gas. Two spin states are present in equal numbers, with field operators $\hat{\psi}_\uparrow(\mathbf{r}, t)$ and $\hat{\psi}_\downarrow(\mathbf{r}, t)$, and the collisional interaction Hamiltonian is approximated by a number of single-particle terms. For convenience, the optical Bragg field is chosen so that it does not flip the particle spin. Implementing the Heisenberg equations of motion and the Bogoliubov transformation,

$$\hat{\psi}_{\uparrow,\downarrow}(\mathbf{r}, t) = \sum_{\mathbf{k}} [u_{\mathbf{k}}(\mathbf{r}, t)\hat{\gamma}_{\mathbf{k}\uparrow,\mathbf{k}\downarrow} \mp v^*_{\mathbf{k}}(\mathbf{r}, t)\hat{\gamma}^\dagger_{\mathbf{k}\downarrow,\mathbf{k}\uparrow}], \quad (1)$$

yields [14–16] the time-dependent Bogoliubov de Gennes equations,

$$i\hbar \frac{\partial}{\partial t}\begin{bmatrix} u_{\mathbf{k}}(\mathbf{r}, t) \\ v_{\mathbf{k}}(\mathbf{r}, t) \end{bmatrix} = \begin{bmatrix} L(\mathbf{r}, t) & \Delta(\mathbf{r}, t) \\ \Delta^*(\mathbf{r}, t) & -L(\mathbf{r}, t) \end{bmatrix}\begin{bmatrix} u_{\mathbf{k}}(\mathbf{r}, t) \\ v_{\mathbf{k}}(\mathbf{r}, t) \end{bmatrix}, \quad (2)$$

where

$$L(\mathbf{r}, t) = -\frac{\hbar^2\nabla^2}{2M} + V_{\text{opt}}(\mathbf{r}, t) - E_F + U(\mathbf{r}, t). \quad (3)$$

The Hartree potential is $U(\mathbf{r}, t) = V\langle\hat{\psi}^\dagger_\alpha(\mathbf{r}, t)\hat{\psi}_\alpha(\mathbf{r}, t)\rangle$, the pair potential is $\Delta(\mathbf{r}, t) = -V\langle\hat{\psi}_\uparrow(\mathbf{r}, t)\hat{\psi}_\downarrow(\mathbf{r}, t)\rangle$, and $u_{\mathbf{k}}(\mathbf{r}, t)$ and $v_{\mathbf{k}}(\mathbf{r}, t)$ are the time-dependent *quasiparticle* amplitudes. We denote the Fermi energy by $E_F = \hbar\omega_F = \hbar^2k_F^2/2M$, the atom mass by M, and the strength of the collisional interaction between fermions by V ($V < 0$). The Bragg field is turned on at $t = 0$ and has the form $V_{\text{opt}}(\mathbf{r}, t) = A\cos(\mathbf{q}\cdot\mathbf{r} - \omega t)/2$, where the wave vector $\mathbf{q}$ is aligned with the x axis.

The description of the collisional interaction in this problem requires a more realistic collisional potential than a contact potential, since we find that Bragg scattering is sensitive to the range of the potential. However, that sensitivity is weak for any realistic range, and we approximate the collisional potential using a contact potential with strength V and momentum space cutoff $\hbar k_c$, where V and k_c are chosen to give the correct scattering length and correct momentum space range. While the static BCS properties are insensitive to k_c [17], the total number of Bragg scattered atoms depends on the value of the cutoff k_c, and in fact the number of pairs scattered vanishes on setting $k_c \to \infty$. Thus, k_c must be chosen finite as above. Full details will be given elsewhere [16].

Full details of our numerical method are beyond the scope of this Letter. Briefly, we have solved Eq. (2) projected onto a momentum space sphere with radius $\hbar k_c$. The initial state is the BCS ground state, i.e., the solution of the time-independent form of Eq. (2) with $V_{\text{opt}} = 0$, which is obtained iteratively. The dynamic evolution of the gas is then determined using a fourth order Runge-Kutta method [18] to solve Eq. (2) for a large number of quasiparticle amplitudes. In principle all quasiparticle modes with momentum components lying inside the momentum space

sphere of radius $\hbar k_c$ should be evolved. However, computational resources limit us to explicitly propagating only quasiparticle modes for which $\mathbf{k}$ lies inside a cylinder oriented along the k_x axis and well within the sphere of cutoff radius k_c. The quasiparticle modes that lie between the cylinder and the surface $|\mathbf{k}| = k_c$ are treated more simply by an approximate method [16]. The size of the cylinder, and the number of quasiparticle modes within it, are chosen to ensure accuracy of the method (e.g., for the results here, approximately 40 000 quasiparticle modes are evolved explicitly).

We consider Bragg scattering of a zero temperature homogeneous Fermi gas. Figures 1(a)–1(c) show the momentum space column density of a Bragg scattered Fermi gas for different Bragg frequencies ω. The column density is $\int n(\mathbf{k}, t)dk_z$, with the number density at momentum $\hbar\mathbf{k}$ given by $n(\mathbf{k}, t) = C\langle\hat{\phi}^\dagger_\alpha(\mathbf{k}, t)\hat{\phi}_\alpha(\mathbf{k}, t)\rangle$, where $\hat{\phi}_\alpha(\mathbf{k}, t) = \int\hat{\psi}_\alpha(\mathbf{r}, t)\exp(-i\mathbf{k}\cdot\mathbf{r})d^3r/(L)^{3/2}$ is the field operator in momentum space, C is a constant chosen such that $\int n(\mathbf{k}, t)d^3k = 1$, and L^3 is the computational volume. The two spin states are scattered identically because of our choice of a spin preserving Bragg field.

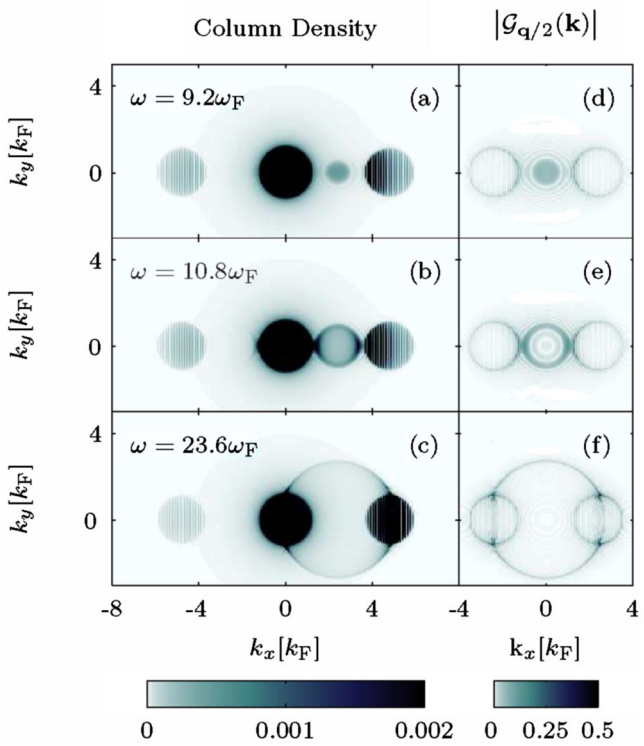

FIG. 1 (color online). Column density and pair correlation function of a Bragg scattered three-dimensional homogeneous Fermi gas at zero temperature. The momentum distribution of the initial cloud is saturated on the chosen scale in order to observe the scattered atoms. Parameters are $A = 1.80E_F$, $q = 4.80k_F$, $t = 8.22/\omega_F$, $k_c = 30k_F$, $k_Fa = -0.427$ [i.e., $U(0) = -0.256E_F$ and $\Delta(0) = 0.049E_F$], and (a),(d) $\omega = 9.20\omega_F$, (b),(e) $\omega = 10.8\omega_F$, and (c),(f) $\omega = 23.6\omega_F$.

The initial cloud, centered at $\mathbf{k} = \mathbf{0}$, has an approximate width given by the modified Fermi wave vector k'_F, defined by $\hbar^2k'^2_F/2M = E_F - U(0)$ (e.g., [19]). In the presence of the Bragg field the atoms scatter by two different mechanisms which we refer to as *single-particle* scattering and *correlated-pair* scattering.

In single-particle Bragg scattering an atom receives a momentum kick of $n\hbar\mathbf{q}$ and energy $n\hbar\omega$, where n is an integer. A resonance condition selects primarily one value of n, and we consider ω in the range of first order Bragg scattering (e.g., [20]), where $n = 1$ is dominant. This results in a cloud of atoms centered at $\mathbf{k} = \mathbf{q}$, as observed in Figs. 1(a)–1(c). A faintly visible cloud at $\mathbf{k} = -\mathbf{q}$ is also observed in Figs. 1(a)–1(c) due to off resonant scattering into the $n = -1$ order. The atom clouds arising from single-particle Bragg scattering would also be observed in the case of Bragg scattering of a noninteracting Fermi gas ($V = 0$).

Figures 1(a)–1(c) also show scattering of atoms into a spherical shell centered at $\mathbf{k} = \mathbf{q}/2$. The atom shell is due to correlated-pair scattering, and is not observed in the case of a noninteracting gas. Correlated-pair scattering has a frequency threshold denoted ω_{thres}, at which atoms are scattered to $\mathbf{k} = \mathbf{q}/2$ [see Fig. 1(a)]. Above threshold [see Figs. 1(b) and 1(c)], the atoms are scattered into a spherical shell and the shell radius increases with Bragg frequency. Atoms scattered into the shell come primarily from the Fermi surface and are correlated about $\mathbf{k} = \mathbf{q}/2$, as demonstrated by the pair correlation function $\mathcal{G}_{\mathbf{q}/2}(\mathbf{k}, t) = \langle\hat{\phi}_\uparrow(\mathbf{q}/2 + \mathbf{k}, t)\hat{\phi}_\downarrow(\mathbf{q}/2 - \mathbf{k}, t)\rangle$, shown in Figs. 1(d)–1(f) for the $k_z = 0$ plane [21]. As well as the ring of correlation due to the scattered pairs, we also observe two rings of radius k'_F centered at $\mathbf{k} = \pm\mathbf{q}/2$, which represent correlation between an atom on the Fermi surface of the initial cloud, and an atom in the single-particle Bragg scattered cloud of order $n = 1$.

We determine the Bragg spectrum of the degenerate Fermi gas by calculating the momentum transfer per atom along the Bragg axis, $\mathcal{P}(t) = \int[\hbar\mathbf{k}\cdot\hat{\mathbf{q}}]n(\mathbf{k}, t)d^3k$, for a range of Bragg frequencies. The Bragg spectrum at zero temperature is given in Fig. 2(a), and is dominated by the broad single-particle resonance familiar from Bragg scattering of a Bose-Einstein condensate (e.g., [20]). The single-particle Bragg resonance is due to two-photon scattering events that scatter atoms by the Bragg momentum $\hbar\mathbf{q}$. The resonance condition is well approximated using energy conservation arguments for noninteracting particles, and by considering an atom scattered from momentum $\hbar\mathbf{k}_R$ to $\hbar(\mathbf{k}_R + \mathbf{q})$ we obtain the resonance condition $\omega_{\text{sp}} = \hbar(q^2 + 2\mathbf{k}_R\cdot\mathbf{q})/2M$. The single-particle resonance [see Fig. 2(a)] is centered at $\omega = \hbar q^2/2M$, and its width is $\delta\omega \approx 2\hbar qk'_F/M + A/\hbar$, where the first term accounts for the momentum width of the initial cloud, and the second term is due to power broadening (e.g., [20]).

Correlated-pair Bragg scattering occurs on the red-detuned side of the single-particle resonance, leading to a

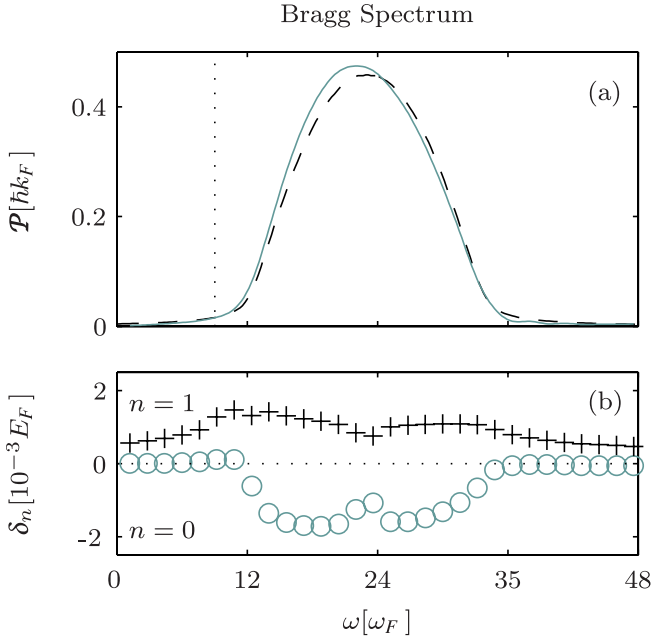

FIG. 2 (color online). (a) Bragg spectrum of a three-dimensional homogeneous Fermi gas at zero temperature. Parameters are $A = 1.80E_F$, $q = 4.80k_F$, $t = 8.22/\omega_F$, $k_c = 30k_F$, and (dashed) $k_F a = 0$ and (solid) $k_F a = -0.427$. The noninteracting case is calculated with the initial momentum width of the gas modified to agree with the interacting case, i.e., $k_F' = 1.12k_F$. The vertical dotted line indicates $\omega = \omega_{\text{thres}}$. (b) Relative change $\delta_n(t) = |\Delta_n(t)| - |\Delta_n(0)|$ of the pair potential Fourier components (+) $n = 1$ and (○) $n = 0$ [see Eq. (5)] for the case $k_F a = -0.427$.

slight asymmetry in the Bragg spectrum [see Fig. 2(a)]. The correlated scattering, which gives rise to the distinctive spherical shell of atoms in momentum space [see Figs. 1(a)–1(c)], depends critically on the presence of Cooper pairs, and can not be understood by the usual single-particle scattering mechanism. Correlated-pair scattering is associated with the formation of a moving grating in the pair potential, which is well approximated by $\Delta(\mathbf{r}, t) \approx \Delta_0(t) + \Delta_1(t)\exp[i(\mathbf{q}\cdot\mathbf{r} - \omega t)]$. The pair potential coefficients Δ_0 and Δ_1, after the Bragg pulse, are shown in Fig. 2(b), where we observe that the homogeneous term Δ_0 is depleted in the region of the single-particle Bragg resonance, while the moving grating amplitude Δ_1, is created over a slightly more extended region. Cooper pairs (of zero center-of-mass momentum) scatter from the moving grating in the pair potential to center-of-mass momentum $\hbar\mathbf{q}$. At threshold [see Fig. 1(a)], the pair potential grating provides just sufficient energy to scatter each atom of a pair to a final momentum $\hbar\mathbf{q}/2$. Above threshold [see Figs. 1(b) and 1(c)], excess energy provided by the pair potential grating is distributed equally between the two atoms of a pair, and the individual momenta of the atoms become $\hbar(\mathbf{q}/2 \pm \mathbf{k}_{\text{rel}})$. A resonance condition for correlated-pair Bragg scattering can be obtained from energy conservation arguments to be $\omega_{\text{pair}} = \hbar(q^2/4 + k_{\text{rel}}^2 - k_F'^2)/M$, which for $k_{\text{rel}} = 0$ gives the threshold frequency $\omega_{\text{thres}} = \hbar q^2/4M - \hbar k_F'^2/M$. Above threshold, the additional kinetic energy $\hbar^2 k_{\text{rel}}^2/2M$ carried by each atom of a scattered pair is given by $\omega - \omega_{\text{thres}} = \hbar k_{\text{rel}}^2/M$, as confirmed by our numerical calculations.

We can understand some important features of Bragg scattering of correlated pairs with an analytic treatment. Because of the periodicity of the Bragg field, the solutions of Eq. (2) have the Bloch form, and can be expanded as

$$u_{\mathbf{k}}(\mathbf{r}, t) = e^{i\mathbf{k}\cdot\mathbf{r}}\sum_n a_n^{\mathbf{k}}(t)e^{in(\mathbf{q}\cdot\mathbf{r}-\omega t)}$$
$$v_{\mathbf{k}}(\mathbf{r}, t) = e^{i\mathbf{k}\cdot\mathbf{r}}\sum_n b_n^{\mathbf{k}}(t)e^{in(\mathbf{q}\cdot\mathbf{r}-\omega t)}, \quad (4)$$

where n is an integer. The self-consistent potentials are periodic, with the translational symmetry of the Bragg field, i.e.,

$$U(\mathbf{r}, t) = \sum_n U_n(t)e^{in(\mathbf{q}\cdot\mathbf{r}-\omega t)}$$
$$\Delta(\mathbf{r}, t) = \sum_n \Delta_n(t)e^{in(\mathbf{q}\cdot\mathbf{r}-\omega t)}. \quad (5)$$

Evolution equations for the coefficients $a_n^{\mathbf{k}}(t)$ and $b_n^{\mathbf{k}}(t)$ can be derived from Eq. (2) to be

$$i\hbar\frac{da_n^{\mathbf{k}}(t)}{dt} = \hbar\omega_n^a(\mathbf{k})a_n^{\mathbf{k}}(t) + \frac{A}{4}[a_{n+1}^{\mathbf{k}}(t) + a_{n-1}^{\mathbf{k}}(t)] + \sum_m U_m(t)a_{n-m}^{\mathbf{k}}(t) + \sum_m \Delta_m(t)b_{n-m}^{\mathbf{k}}(t), \quad (6)$$

and

$$i\hbar\frac{db_n^{\mathbf{k}}(t)}{dt} = \hbar\omega_n^b(\mathbf{k})b_n^{\mathbf{k}}(t) - \frac{A}{4}[b_{n+1}^{\mathbf{k}}(t) + b_{n-1}^{\mathbf{k}}(t)] - \sum_m U_m(t)b_{n-m}^{\mathbf{k}}(t) + \sum_m \Delta_m^*(t)a_{n+m}^{\mathbf{k}}(t), \quad (7)$$

where $\hbar\omega_n^{a,b}(\mathbf{k}) = \pm[\hbar^2(\mathbf{k} + n\mathbf{q})^2/2M - E_F] - n\hbar\omega$. Initially the only nonzero coefficients are $a_0^{\mathbf{k}}$ (for $|\mathbf{k}| \gtrsim k_F'$) and $b_0^{\mathbf{k}}$ (for $|\mathbf{k}| \lesssim k_F'$). The mean-field coefficients U_m and Δ_m must be obtained self-consistently, in particular

$$\Delta_m(t) = -\bar{V}\sum_{\mathbf{k}}\sum_n a_n^{\mathbf{k}}(t)b_{n-m}^{\mathbf{k}*}(t), \quad (8)$$

with $\bar{V} = T/(1 - \alpha T)$, where T is the low energy T-matrix and $\alpha = Mk_c/2\pi^2\hbar^2$ [16,17].

First order correlated-pair Bragg scattering is mediated by a moving grating in the pair potential, arising due to terms $m = 1$, $n = 0, 1$ in Eq. (8) becoming nonzero. Those terms are seeded by single-particle Bragg scattering events in which an atom on the Fermi surface is scattered by momentum $\hbar\mathbf{q}$. It can be shown, from Eqs. (6) and (7), that single-particle transitions generate coefficients $a_1^{\mathbf{k}}$ (for $|\mathbf{k}| \gtrsim k_F'$) and $b_{-1}^{\mathbf{k}}$ (for $|\mathbf{k}| \lesssim k_F'$). In the region of the Fermi surface, $|\mathbf{k}| \approx k_F'$, Δ_1 is generated due to the formation of contributions $a_1^{\mathbf{k}}b_0^{\mathbf{k}*}$ and $a_0^{\mathbf{k}}b_{-1}^{\mathbf{k}*}$. Physically that corresponds to seeding pair correlations about $\mathbf{k} = \mathbf{q}/2$.

When an atom with momentum $\hbar\mathbf{k}_R \approx \hbar k'_F \hat{\mathbf{k}}_R$, is scattered by a single-particle transition to $\hbar(\mathbf{k}_R + \mathbf{q})$, it remains correlated with its unscattered pair at momentum $-\hbar\mathbf{k}_R$. That reduces the system pairing about $\mathbf{k} = \mathbf{0}$ (Δ_0), and generates a pair correlation about $\mathbf{k} = \mathbf{q}/2$ (Δ_1) [see Fig. 2(b)]. The correlation seeding can also be observed in $\mathcal{G}_{\mathbf{q}/2}(\mathbf{k}, t)$ [see Figs. 1(d)–1(f)], where a point on the left most circle represents correlation between an atom on the Fermi surface of the initial cloud and its pair which has been scattered by $\mathbf{q}$.

Following the initiation of the pair potential grating, its subsequent development can be understood in terms of a truncated version of Eqs. (6) and (7), i.e.,

$$i\hbar \frac{d}{dt}\begin{bmatrix} a_0^{\mathbf{k}}(t) \\ b_{-1}^{\mathbf{k}}(t) \end{bmatrix} = \begin{bmatrix} \epsilon_0^a(\mathbf{k}) & \Delta_1(t) \\ \Delta_1^*(t) & \epsilon_{-1}^b(\mathbf{k}) \end{bmatrix}\begin{bmatrix} a_0^{\mathbf{k}}(t) \\ b_{-1}^{\mathbf{k}}(t) \end{bmatrix}, \quad (9)$$

which is appropriate for describing the scattered pairs. In Eq. (9), $\epsilon_n^{a,b}(\mathbf{k}) = \hbar\omega_n^{a,b}(\mathbf{k}) \pm U_0$, and $\Delta_1(t) = -\bar{V}\sum_{\mathbf{k}} a_0^{\mathbf{k}}(t) b_{-1}^{\mathbf{k}*}(t)$. The term $a_0^{\mathbf{k}} b_{-1}^{\mathbf{k}*}$ becomes significant only if $\epsilon = \epsilon_0^a(\mathbf{k}) - \epsilon_{-1}^b(\mathbf{k}) \approx 0$, i.e., when correlated scattering transitions conserve energy ($\omega \geq \omega_{\text{thres}}$). At threshold, the summands in Δ_1 have a stationary phase, leading to enhancement of the grating amplitude Δ_1 [see Fig. 2(b)]. The thickness δk of the spherical shell of scattered pairs can be estimated by assuming a frequency width Γ, determined by the Bragg pulse length ($\Gamma \approx \pi/t$), and setting $\delta\epsilon = \hbar\Gamma$, to find that $\delta k \approx (\pi M/\hbar t + k_{\text{rel}}^2)^{1/2} - k_{\text{rel}}$.

We have investigated the dependence of correlated-pair Bragg scattering on a range of system parameters. In Fig. 1(b), $\sim$0.2% of the atoms are scattered by correlated-pair Bragg scattering, and the number of scattered pairs grows linearly with the length of the Bragg pulse (until $t \sim 70/\omega_F$). Over the range $-0.18 \geq k_F a \geq -0.69$, the number of pairs scattered increases quadratically with $\Delta(0)$ indicating the coherent nature of the scattering process. For $k_F a = -0.689$ [all other parameters as per Fig. 1(b)] there are $\sim$6% scattered pairs. However, we emphasize that for $|k_F a| \gtrsim 1$ the mean-field approach may not be quantitatively accurate (e.g., [12,22]). The number of correlated pairs scattered can be further increased by enhancing the single-particle scattering processes that seed the pair potential grating, either by increasing the Bragg field strength A, or by reducing the Bragg wave vector $\mathbf{q}$ (to make the seeding more resonant).

In conclusion, we have calculated solutions of the time-dependent Bogoliubov de Gennes equations for a zero temperature homogeneous three-dimensional Bragg scattered Fermi gas, in the regime where the momentum transfer is well outside the Fermi surface. We predict Bragg scattering of correlated atom pairs, which has a distinctive signature in momentum space, namely, a spherical shell of atoms centered at half the usual Bragg momentum transfer. Correlated-pair Bragg scattering occurs via a Bragg grating formed in the pair potential, and has a well-defined frequency threshold on the red-detuned side of the familiar single-particle Bragg resonance. We have developed an analytic model that explains the mechanism by which the pair potential grating is generated, and observe that the number of scattered pairs is proportional to the square of the initial pairing field.

This work was supported by Marsden Fund No. UOO0509 and the Tertiary Education Commision (No. TAD 884).

[1] M. Kozuma, L. Deng, E. W. Hagley, J. Wen, R. Lutwak, K. Helmerson, S. L. Rolston, and W. D. Phillips, Phys. Rev. Lett. **82**, 871 (1999).
[2] D. M. Stamper-Kurn, A. P. Chikkatur, A. Görlitz, S. Inouye, S. Gupta, D. E. Pritchard, and W. Ketterle, Phys. Rev. Lett. **83**, 2876 (1999).
[3] K. Bongs, S. Burger, D. Hellweg, M. Kottke, S. Dettmer, T. Rinkleff, L. Cacciapuoti, J. Arlt, K. Sengstock, and W. Ertmer, J. Opt. B **5**, S124 (2003).
[4] S. Richard, F. Gerbier, J. H. Thywissen, M. Hugbart, P. Bouyer, and A. Aspect, Phys. Rev. Lett. **91**, 010405 (2003).
[5] R. Geursen, N. R. Thomas, and A. C. Wilson, Phys. Rev. A **68**, 043611 (2003).
[6] S. R. Muniz, D. S. Naik, and C. Raman, Phys. Rev. A **73**, 041605(R) (2006).
[7] J. Ruostekoski, Phys. Rev. A **61**, 033605 (2000).
[8] A. Minguzzi, G. Ferrari, and Y. Castin, Eur. Phys. J. D **17**, 49 (2001)
[9] M. Rodriguez and P. Törmä, Phys. Rev. A **66**, 033601 (2002).
[10] H. P. Büchler, P. Zoller, and W. Zwerger, Phys. Rev. Lett. **93**, 080401 (2004).
[11] B. Deb, J. Phys. B **39**, 529 (2006).
[12] R. Combescot, S. Giorgini, and S. Stringari, Europhys. Lett. **75**, 695 (2006).
[13] P. B. Blakie, R. J. Ballagh, and C. W. Gardiner, Phys. Rev. A **65**, 033602 (2002).
[14] P. G. de Gennes, *Superconductivity of Metals and Alloys* (W. A. Benjamin, Inc., New York, 1966).
[15] J. B. Ketterson and S. N. Song, *Superconductivity* (Cambridge University Press, Cambridge, 1999).
[16] K. J. Challis, R. J. Ballagh, and C. W. Gardiner (to be published).
[17] M. L. Chiofalo, S. J. J. M. F. Kokkelmans, J. N. Milstein, and M. J. Holland, Phys. Rev. Lett. **88**, 090402 (2002).
[18] R. J. Ballagh, Computational Methods for Nonlinear Partial Differential Equations, http://www.physics.otago.ac.nz (2000).
[19] N. Nygaard, G. M. Bruun, C. W. Clark, and D. L. Feder, Phys. Rev. Lett. **90**, 210402 (2003).
[20] P. B. Blakie and R. J. Ballagh, J. Phys. B **33**, 3961 (2000).
[21] The maximum possible correlation for a pair of atoms with momenta $\pm\hbar\mathbf{k}$ is $|\mathcal{G}_{\mathbf{0}}(\mathbf{k}, t)| = \frac{1}{2}$.
[22] J. R. Engelbrecht, M. Randeria, and C. A. R. Sá de Melo, Phys. Rev. B **55**, 15 153 (1997).